Physical Modelling for Hallstatt Archaeology

Bernhard Heinzl[1 *], Erik Auer[2], Bernhard Slowacki[2], Kerstin Kowarik[3], Hans Reschreiter[3], Nikolas Popper[1], Felix Breitenecker[2]

[1] dwh Simulation Services, Neustiftgasse 57-59, 1070 Vienna, Austria; **bernhard.heinzl@dwh.at*
[2] Institute for Analysis and Scientific Computing, Vienna Univ. Technology, Vienna, Austria
[3] Natural History Museum Vienna, Burgring 7, 1010 Vienna, Austria

Abstract. Computer simulation can contribute important insights into different areas of archaeology as an addition to traditional experimental methods used to find answers for certain questions arising from archaeological findings, e.g. how tools were used or simply why things were the way they were. In a cooperative project between the Natural History Museum Vienna and the Vienna University of Technology, questions regarding prehistoric physical systems are analyzed. These systems originate from archaeological investigations on the prehistoric salt mines in Hallstatt (Austria) in the Bronze Age.
Three case studies are presented in this article. The first example studies different designs of rope pull systems used to hoist the broken salt from the mining halls through shafts to the surface. In the second task, bronze picks for breaking the salt are investigated using dynamic simulation. The third and last task presents some calculations regarding illumination and air consumption in the mining halls. The simulations allow comparison of different scenarios, help falsifying propositions and gain knowledge in certain aspects regarding technical equipment and working conditions in the prehistoric salt mines in Hallstatt.

Introduction

The prehistoric salt mines of Hallstatt in Austria are subject of great interest for archaeologists, not only for their technological aspects, but also for their complex economic structure. Salt mining activities are dated to 1458-1245 B.C. in the Bronze Age [1].

A large amount of archaeological findings of technical equipment and organic materials (timber, wooden tools, strings of bast, fur etc.) and the perfect conditions of preservation in the mines due to the conserving properties of salt allow for a reconstruction of the working process in the mines [2].

Archaeologists develop a technological reconstruction in form of a mental model (see Figure 1). This mental model suggests that mining was organized in an efficient, nearly industrial manner with highly specialized tools. Salt was mined in underground mining chambers using special bronze picks. The broken salt was collected in buckets and carried to the vertical shaft where it was hoisted to the surface using a wool sack or cloth attached to a linden bast rope.

The high degree of specialization and functionality observable on certain tools and the design for high efficiency suggest that the workforce had highly specialized knowledge in mining technology and infrastructural processes [2].

This mental model raises further questions, which need to be formalized and are typically investigated in experiments using reconstructions of prehistoric tools and utilities. As a new approach, computer simulation can also help to gain knowledge about technological issues and quantitatively compare different possibilities. Results of this work (experiments and simulation) and their interpretation then allow archaeologists to make conclusions about the technological concept and together with new excavation findings update their mental model leading to an iterative process. This process is visualized in Figure 2.

As part of a collaboration between the Natural History Museum Vienna and the Vienna University of Technology, several questions from this mental model regarding technical equipment and utilities in the Hallstatt salt mines are formalized and investigated using software tools for modelling and simulation of physical systems. Different scenarios are considered and comparisons are quantified in order to be able to evaluate the different possibilities regarding their plausibility and eligibility.

SNE Simulation Notes Europe – Print ISSN 2305-9974 | Online ISSN 2306-0271
SNE 22(1), 2012, 25-32 | doi: 10.11128/sne.22.tn.10109

Figure 1. Impression of a Bronze Age mining hall as reconstructed for the Christian v. Tusch-Werk in Hallstatt (© D. Gröbner, H. Reschreiter, NHM Vienna). The workers used special bronze picks to break the salt. The salt pieces were then collected in buckets and carried to a vertical shaft where it was hoisted to the surface using a rope pull system. Burning woodchips served as illumination in the underground mining halls.

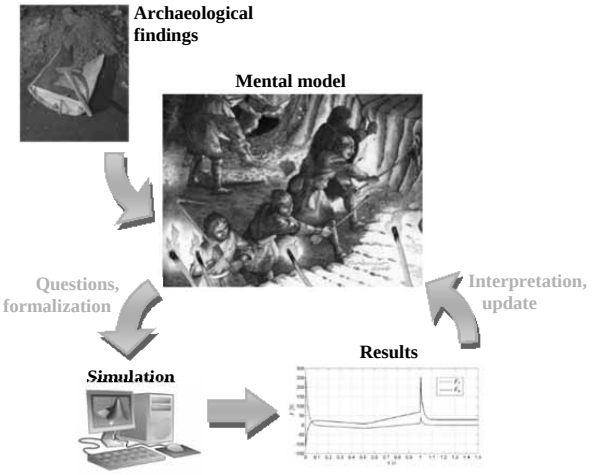

Figure 2. Iterative process for adapting the mental model. New archaeological findings provide information. Questions arising from the mental model are formalized and mapped into a computer model. Simulation then generates results for different scenarios, which are interpreted and allow conclusions for the mental model (© A. Rausch, D. Gröbner, H. Reschreiter, NHM Vienna).

1 Rope Pull Systems

Rope pull systems were used to hoist the broken salt from the mining halls through shafts to the surface [2] (see Figure 3). While there are archaeological findings of bast ropes and other appliances, there are still some matters regarding the construction, length and arrangement of the rope pull systems at issue.

To estimate and compare the time and strength requirements for transporting the salt, various options are analyzed using simulation models. For example, we compare two variants of the rope design, an open and a closed version, depicted in Figure 4.

An important issue also concerns modelling of the rope guide, for which we consider two possibilities, one with sliding friction on a log and one with return pulley.

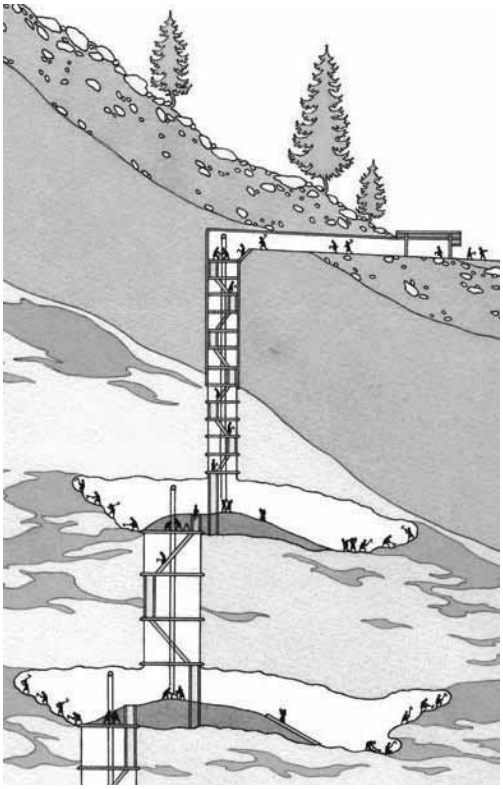

Figure 3. Schematic reconstruction of the mining halls and shaft structure with rope pull systems (© D. Gröbner, H. Reschreiter, NHM Vienna).

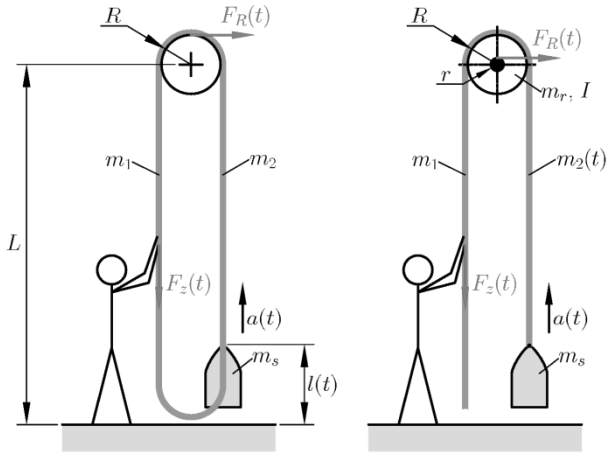

Figure 4. Different design options for the rope pull system with closed rope (left) or open rope (right). The schematic also shows two possibilities for the rope guide: sliding friction on a log (left) and rotating return pulley (right).

1.1 Rope Guide on a Log

Considering simple balance of forces according to Figure 4 taking into account mass of the rope on both sides (m_1 and m_2, resp.) and forces of inertia leads to

$$F_z(t) + m_1(g - \mathrm{a(t)}) - F_R(t) = m_2(t)\big(g + a(t)\big) + m_s\big(g + a(t)\big) \quad (1)$$

with the external force $F_z(t)$, predefined acceleration $a(t)$ (see equation (4)), acceleration of gravity g and mass of the salt bags m_s. The coulomb friction force $F_R(t)$ is given as

$$F_R(t) = \mu(v(t))[F_z(t) + m_1\big(g - a(t)\big) + m_2(t)(g + a(t)) + m_s\big(g + a(t)\big)]. \quad (2)$$

The expression in square brackets denotes the total normal force on the log. For the friction coefficient μ, we define the following expression depending on the rope velocity v, also visualized in Figure 5.

$$\mu(v) = (\mu_c + (\mu_{\mathrm{brk}} - \mu_c)\exp(-c_v|v|)\,\mathrm{sgn}(v) + fv \quad (3)$$

with a coulomb friction coefficient μ_c, breakaway friction coefficient μ_{brk}, viscous friction coefficient f and coefficient c_v. This friction model takes into account sticking friction at velocities near zero (μ_{brk}) as well as viscous friction at high velocities (fv).

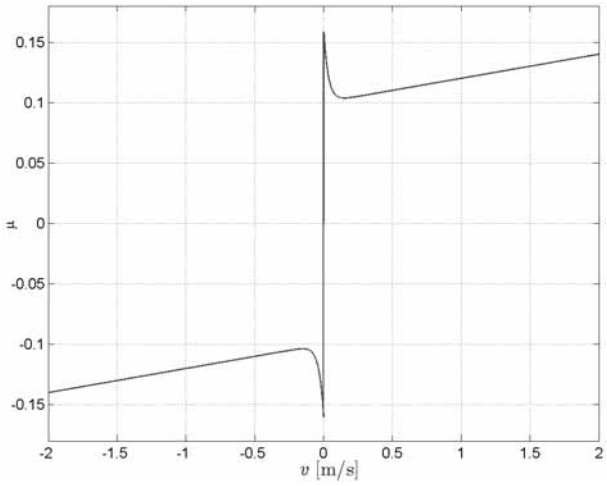

Figure 5. Model of the friction coefficient μ with sticking and viscous components for parameters $\mu_c = 0.1$, $\mu_{\mathrm{brk}} = 0.16$, $c_v = 30$ and $f = 1/50$.

In order to determine the force necessary for hoisting the salt to the surface, the proposed model receives the desired velocity over time as input signal and calculates the necessary external force $F_z(t)$. One possible input signal is depicted in Figure 6. It shows a smooth nearly periodic signal (due to alternating pull of a single person) with global upward trend.

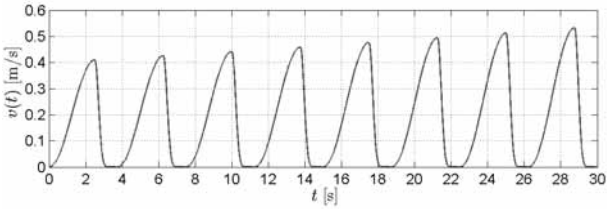

Figure 6. Possible input signal $v(t)$ with smooth progression and global upward trend.

The external force can then be calculated using equations (1), (2) and (3) and the time derivative

$$a(t) = \frac{d}{dt} v(t) \tag{4}$$

of the input velocity. For an open rope, the mass $m_2(t)$ of the rope on the right side of the log depends on the current position $l(t)$,

$$m_2(t) = m_{2,0} - \rho l(t), \tag{5}$$

with the assumed density $\rho = 1.5$ kg/m and starting mass $m_{2,0} = \rho L$, and therefore decreases over time according to

$$\frac{d}{dt} m_2(t) = -\rho \frac{d}{dt} l(t) = -\rho v(t) \tag{6}$$

with given input velocity. If the rope is closed (see Figure 4 left), then the mass m_2 is constant

$$m_2 = \rho L. \tag{7}$$

In both cases (open and closed rope), the mass m_1 on the left side is assumed constant, also with

$$m_1 = \rho L. \tag{8}$$

The mass of one bag of salt is assumed to be about 28 kg which corresponds to a volume of 20 l. For the value of m_s, one or more bags of salt are considered,

$$m_s = k \cdot 28 \text{ kg}, \quad k = 1,2,3, \ldots \tag{9}$$

with the number of bags k.

Evaluation of a simulation using the presented equations implemented in MATLAB and parameters $L = 20$ m, $k = 1$ for example for a greased log ($\mu_c = 0.1$, $\mu_{\text{brk}} = 0.16$) provide the results given in Figure 7. The results show a total duration of about 81 s to hoist one bag of salt over a height of 20 m, maximum external force is about 500 N. The height $l(t)$ pulsates due to the periodic velocity (see Figure 6).

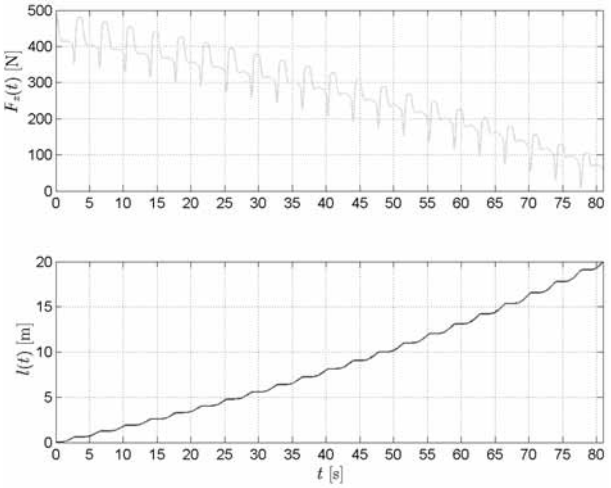

Figure 7. Simulation results for a greased log with open rope and $L = 20$ m, $k = 1$.

Similar investigations for different shaft heights L as well as different number of bags lead to the results presented in Figure 8. It shows that each additional bag of salt adds about 400 N to the external force, which is more than the own weight because of additional friction.

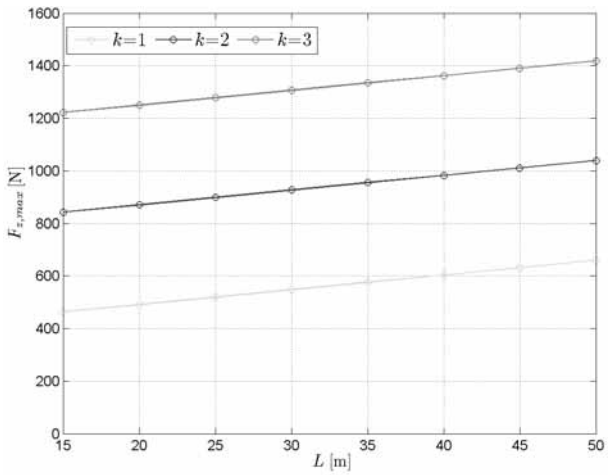

Figure 8. Maximum external force F_z for the scenario with log for different shaft heights L and different number of bags k.

1.2 Rope Guide with Rotating Return Pulley

Using a return pulley with outer Radius R and axle radius r instead of a static log adds terms for pulley mass m_r and inertia I to equations (1) and (2), thus, with regard to Figure 4, resulting in the equations

$$F_z(t) + m_1(g - \mathrm{a(t)}) - F_R(t)\frac{\mathrm{r}}{\mathrm{R}} - \frac{Ia(t)}{\mathrm{R}^2} = m_2(t)(g + a(t)) + m_s(g + a(t)), \tag{10}$$

$$F_R(t) = \mu(v(t))[F_z(t) + m_1\big(g - a(t)\big) + m_2(t)\big(g + a(t)\big) + m_s\big(g + a(t)\big) + m_r]. \quad (11)$$

Different values can be considered for the parameters of the pulley depending on its material (wood, bronze, etc.). For a pulley made of wood we get for example the following parameters:

$$R = 0.6\text{ m},\ r = 0.2\text{ m},\ m_r = 16.3\text{ kg},\ I = 3.3\text{ kgm}^2,\ \mu_c = 0.06,\ \mu_{\text{brk}} = 0.11. \quad (12)$$

As a simulation result, maximum required external force F_z for the scenario with return pulley and different values for shaft height L and number of bags k is presented in Figure 9. Comparison with Figure 8 shows significant reduced force requirement due to lower friction.

Figure 10 compares force input between the version with open rope and with closed rope (i.e. where both ends are connected). Since the moving mass is constant for the variant with closed rope, the required force is also constant in average, whereas in the other case the average decreases steadily over time. A closed rope enables more uniform distribution of the rope mass and therefore requires less external force.

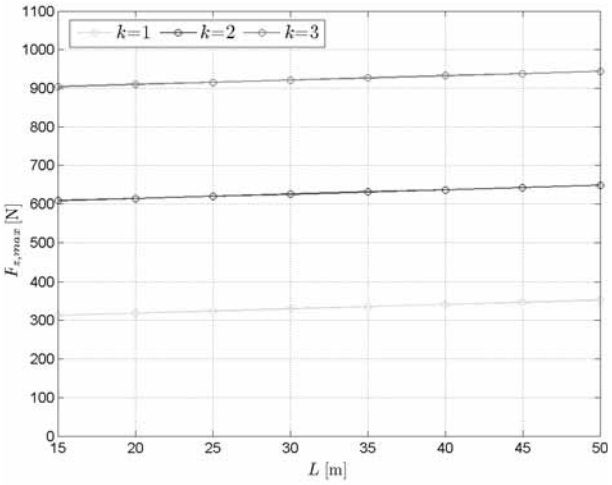

Figure 9. Maximum external force F_z for the scenario with return pulley for different shaft height L and different number of bags k.

In summary the simulation results show significant force requirement for the model with sliding friction, especially because of the high mass of the rope. This is also the reason for limitations regarding the maximum allowed shaft height.

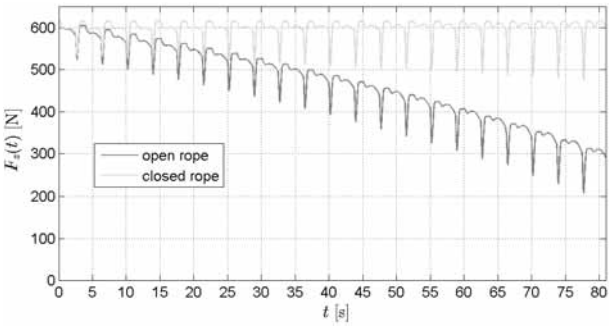

Figure 10. External force $F_z(t)$ over time for the scenario with return pulley and both variants of rope design.

With the presented equations it is also possible to provide the external force $F_z(t)$ as an input signal and calculate resulting velocity $v(t)$ and position $l(t)$ over time. This is still ongoing work and will be investigated in further studies.

2 Bronze Picks

Archaeologists know from excavation findings that the salt was mined using bronze picks with wooden handle [2] (see Figure 11 left). Highly interesting is the unusual shape of these picks with a typical angle between the shaft and tip of about 55 to 75 degrees. It is believed that this particular shape was adapted to the specific working conditions in the Hallstatt mines, especially since no similar devices have been found at other at archaeological sites. The small angle does not allow typical circular hacking motion, which is why it is not yet completely clear exactly how such a pick was used.

Modelling the pick as a rigid body system (Figure 11 right) allows dynamic simulation and evaluating possible movement scenarios and comparisons regarding acceleration and reaction forces.

Different usage of the pick can be considered, e.g. breaking the salt on the wall or on the floor, different grip points, using one or two hands, etc. Figure 12 shows a visualization of a wall impact as an example scenario presented in this article.

An object-oriented modelling approach for mechanical rigid multibody systems (in our case using MATLAB/SimMechanics [3]) allows quick and intuitive structured model development using predefined components. Dynamic and constraint equations are generated, sorted and processed for numeric simulation automatically by the software, allowing easy adaption to different scenarios, e.g. forward or inverse dynamics.

Figure 11. Left: Reconstructed Bronze Age pick (© A. Rausch, NHM Vienna). Right: Rigid body model of the pick in MATLAB/SimMechanics.

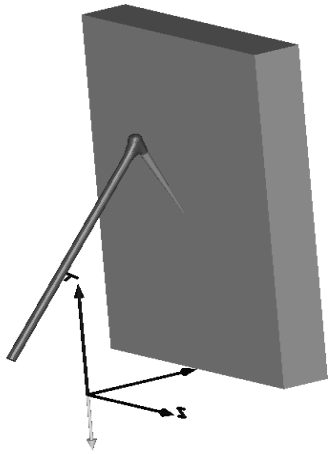

Figure 12. Visualization of an example scenario, where the pick breaks salt off a wall located at $x = 0.5$ m.

Figure 13 depicts the rigid body model for the pick developed in MATLAB/SimMechanics. Two phases are considered:

- During free motion (block 'Acceleration'), the pick accelerates along a fixed trajectory.
- When collision with the wall is detected, the actuation switches to the block 'Collision', and the body decelerates until it comes to a stop.

The pick has three degrees of freedom - two translational (x and y) and one rotational (phi, along the z-axis). Sensor elements allow measuring acceleration as well as reaction forces.

Movement trajectories are obtained by geometrical considerations like shown in Figure 14. Several points are defined along a trajectory of the tool tip depending on the range of motion for a human. Taking into account the time relation, this trajectory also determines velocity and acceleration behaviour. Coordinates for one example trajectory are presented in Figure 15.

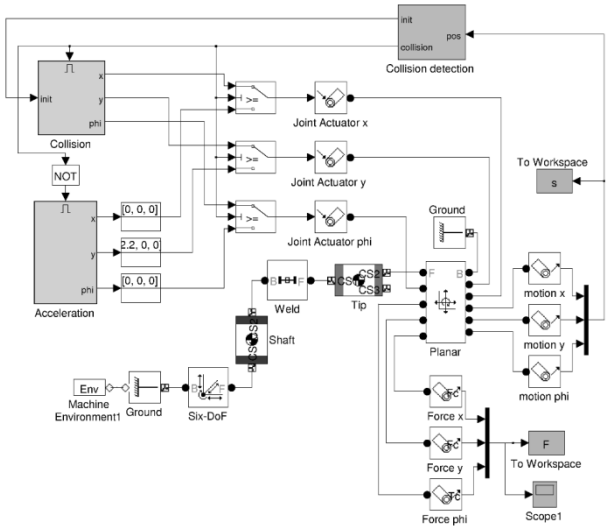

Figure 13. Rigid body model for the bronze pick in MATLAB/SimMechanics. Motion actuation is switched between two states: During free motion (block 'Acceleration'), movement is restricted along a predefined trajectory. After the impact, the tip decelerates until standstill (block 'Collision').

Special focus has to be put on the angle in which the tool tip hits the wall. In order to use the tool effectively (this results from the shape of the tip), the impact angle is required to be

$$\alpha = 20° \ldots 30°. \tag{13}$$

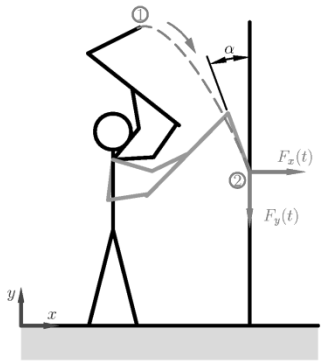

Figure 14. Trajectory for movement of the tool tip and reaction forces F_x and F_y.

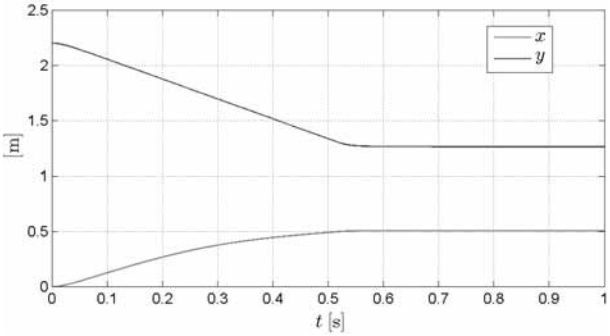

Figure 15. x- and y-coordinates over time for an example trajectory.

Using this geometry data as well as mass and inertia calculations for shaft and tip, the rigid body model can be set up. Simulation provided by inverse dynamics features of the simulator then calculates for example reaction forces (F_x, F_y) on the tool tip, see Figure 16.

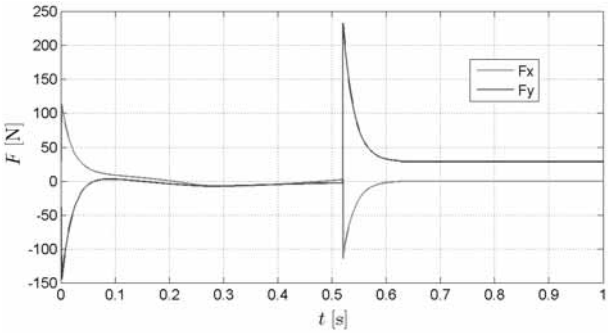

Figure 16. Reaction forces in x- and y-direction on the tool tip as a simulation result for the presented scenario. At $t = 0.52$ s, the impact on the wall occurs leading to a peak in the vertical force.

Other scenarios like mining the salt on horizontal or inclined surfaces are also currently investigated. However, it already shows that mining on the floor seems more exhausting, requires more energy and is therefore less efficient than mining on the wall.

3 Woodchip Flame, Lighting and Air Consumption

During mining, burning sticks of wood served as the only illumination in the mining halls (see also Figure 1). Burnt down woodchips were found during excavation in large quantities [2].

The resulting light intensity depending on the number of burning woodchips can be estimated using a uniform arrangement shown in Figure 17. The flame of a burning woodchip is comparable to a flame of a burning candle, therefore we assume a light intensity for each flame of

$$I_v = 1 \text{ cd}. \tag{14}$$

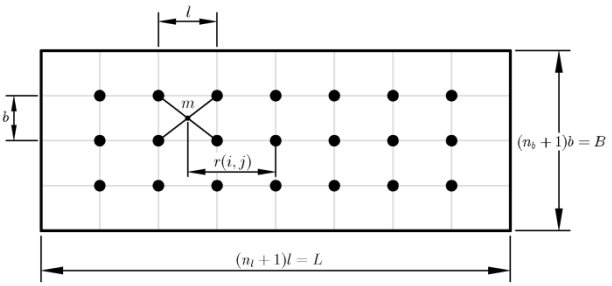

Figure 17. Uniform arrangement of burning woodchips (n_l in length, n_b in width) in a rectangular mining hall.

Local minimum illumination occurs at points of maximum distance to the light sources (for example point m in Figure 17). For such a point, the distance $r(i,j)$ to each woodchip can be calculated:

$$r(i,j) = \sqrt{((i-1)l + \frac{l}{2})^2 + ((j-1)b + \frac{b}{2})^2} \tag{15}$$

and the sum over all positions leads to the total illuminance

$$E_{v,m} = \sum_{i=1}^{n_l} \sum_{j=1}^{n_b} \frac{I_v}{r(i,j)^2}. \tag{16}$$

For different densities of woodchips in length and width,

$$\rho_l = \frac{n_l}{L}, \quad \rho_b = \frac{n_b}{B}, \tag{17}$$

calculation results are shown in Figure 18.

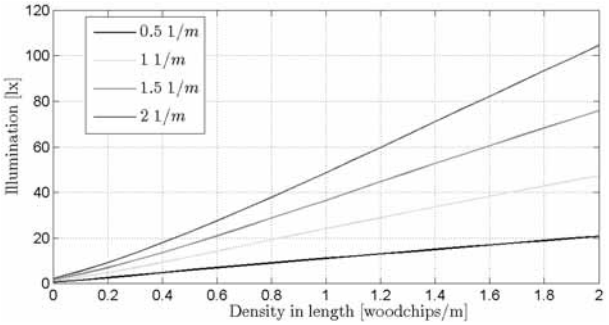

Figure 18. Calculation results for illumination for different densities of woodchips in length and width.

Furthermore, some static calculations help estimating the oxygen consumption of the flames, which, in addition to the oxygen demand of the workers, give information about the necessary air ventilation. For the air consumption of a person doing heavy labour, we assume a typical value of

$$A_p = 0.81 \frac{\mathrm{m}^3}{\mathrm{h}} \tag{18}$$

at 21% percentage of oxygen in the air. A typical woodchip made of fir wood consumes about

$$A_w = 0.014\ \mathrm{m}^3 \tag{19}$$

of oxygen during burning. Altogether, this data leads to the following formula for the total air consumption:

$$A_{\text{total}} = kA_p + n\frac{A_w}{21\% \cdot T} \tag{20}$$

with the number of workers k, total number of woodchips n ($n = n_l \cdot n_b$) and burning time T of a woodchip. Figure 19 depicts calculation results for different parameter values.

This air consumption represents the minimum necessary air exchange in the mining halls for a certain illumination in order to keep the oxygen level constant.

Future work will focus on fluid simulations for the air distribution in the underground mining halls and shaft system in order to determine possible air change rates and - combined with the results above - quantify limitations regarding maximum number of workers in the mining halls.

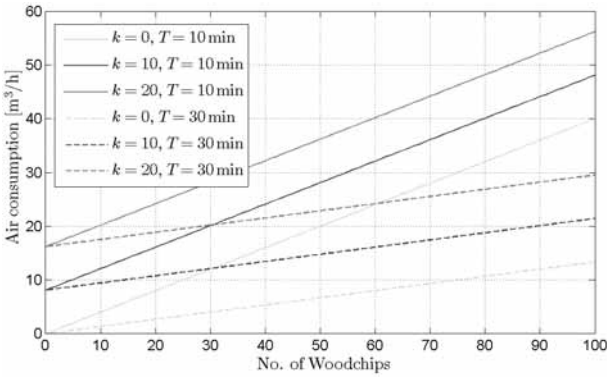

Figure 19. Calculation results for air consumption for different number of woodchips, burning time T and workers k.

4 Conclusion

The presented simulations provide quantitative results for different scenarios and experiments in order to assess their plausibility. Even though the results may not produce many definitive answers for archaeologists, it still allows falsifying certain propositions and thus restricts the total set of possibilities.

Therefore, modelling and simulation concludes to be a useful tool in experimental archaeology which can be nicely combined with physical experiments (a method which is quite common in archaeology) in order to obtain data input and parameter values for the simulation.

The calculations and simulation results are visualized graphically. Their evaluation and interpretation helps archaeologists gain knowledge about transport mechanisms and working conditions in the prehistoric salt mines in Hallstatt and in conclusion adapt and refine the mental models in an iterative process.

New object-oriented modelling approaches for physical systems enable the user to develop modular models in a structural manner, which can easily be adapted to different scenarios.

References

[1] M. Grabner, H. Reschreiter, F.E. Barth, A. Klein, D. Geihofer, R. Wimmer. *Die Dendrochronologie in Hallstatt*. Archäologie Österreichs, 17(1): 49-58, 2006.

[2] H. Reschreiter, K. Kowarik. The Bronze Age. In: Kern et al. *Kingdom of Salt: 7000 Years of Hallstatt.* Vienna: VPA3, Natural History Museum Vienna, 48-64, 2009.

[3] MathWorks, Inc. *SimMechanics User's Guide*. 2011. Available online: http://www.mathworks.de/help/pdf_doc/physmod/mech/mech_ug.pdf

Submitted: January 2012
Revised: February 10, 2012
Accepted: March 20, 2012